SCIENTIFIC REPORT

Dynamic molecular resolution imaging of preocular fluid impressions

M Berry, D Brayshaw, T J McMaster

Br J Ophthalmol 2004;**88**:1460–1466. doi: 10.1136/bjo.2003.040121

Aim: The preocular fluid is renewed with molecules secreted by the underlying cells and with lacrimal gland secretions, while maintaining a stable surface topography. The authors tested the hypothesis that interactions between gelled and newly inserted mucins are the key to this stability.

Methods: Using atomic force microscopy, the authors studied the topography of the freshly isolated preocular fluid obtained by impression cytology. The effects of adding mucins to this impression were compared with adding mucins to a pure mucin macromolecular assembly as a single component control to the more complex preocular fluid. The control structure was built up by repeated addition of pure ocular mucin to a tethering surface.

Results: Imaging at molecular resolution showed a thin layer of superficial preocular fluid with an appearance consistent with a gel that was very flat, with surface roughness of approximately 0.1 nm. Mucin molecules adhering to a clean flat surface maintained their individual character when overlapping, whereas molecules integrating in the impression could not be followed individually. Both the preocular impression and the pure mucin assembly were stable under imaging for at least 90 minutes. The roughness of the pure mucin network decreased as more mucin was added. In contrast, there was a small increase in the roughness of the 2.25 μm^2 area of impression over the 60 minutes of continuous imaging, although locally there appeared to be infill of low height features. Disulphide bond breaking resulted in the collapse of the imaged structure in both the pure mucin control and the more complex ex vivo preocular impression.

Conclusions: Polymeric mucins linked by disulphide bonds prevent or lessen loss of ocular surface material into the surrounding aqueous tears.

A number of models have been offered for the structure of tears, without yet reaching a consensus on either makeup or thickness.[1–4] A continuous fluid, dominated by mucins immediately adjoining the epithelial cells, and with structure on all scales, is a current working model. The contributions of tear glycoconjugates, proteins, and lipids to structure and function, and the interplay between these components, are still to be fully understood.

Macroscopic observation of the tear film—for example, from interference fringes,[5] reveals surface features that remain unchanged through a number of blinks. Yet the preocular fluid is renewed continuously with molecules, added both from the epithelium it overlays and from the lacrimal gland, that integrate seamlessly into the preocular fluid.

A normal tear film smoothes over the imperfections of the ocular surface and improves its optical quality; visual acuity in dry eye patients is increased after instillation of artificial tears.[6] To achieve this function, the surface of the preocular fluid should be flat over extended areas, and the scale of its surface features should be smaller than the wavelength of light.

Atomic force microscopy (AFM) is a technique where an atomically sharp probe (the tip) attached to a flexible force sensing beam (the cantilever) interacts physically with the sample under inspection. It has been used very successfully with biological materials, as it will operate in a physiological environment.[7] We used AFM to image the hydrated preocular fluid collected directly on mica to determine whether its appearance is consistent with that of a gel.[4 8–10] The strategy we adopted was to obtain a very thin impression, which mirrored the features on the actual surface of the preocular fluid. In parallel we followed the formation of a pure mucin network, as a single component control, the top surface of which we imaged throughout.

Preocular impressions present possibly the ultimate challenge to AFM imaging, where a mechanical interaction with the sample is required. Macromolecular polysaccharide assemblies, characterised by a low solid volume fraction and cross links of covalent or physical origin,[11 12] are mechanically very soft, and hence the typical resolution in AFM images is of the order of microns, rather than nanometres. This is in marked contrast to the resolution of single glycoprotein molecules at the subnanometre level.[13–15]

When an AFM cantilever is oscillated in liquid, the natural resonance of the oscillation is damped leading to a decrease in the quality factor (Q-factor) of the resonance. The most pertinent outcome is that the force applied by the cantilever each time it taps the surface is of the order of nanoNewtons (nN), sufficiently high to deform the sample.[16] By applying an electronic feedback technique,[17] it is possible to lessen the damping of the cantilever, decrease the interaction force during each tap, and consequently increase the spatial resolution. The benefits of observing a real gel surface at nanometre resolution via manipulation of the cantilever resonance opens up the possibility of following real time developments in the labile surface, including molecular level interactions.

It is known that concentrations of pure mucins up to 20 times higher than physiological are needed in vitro to duplicate the in vivo properties of their solutions.[18 19] We used purified ocular mucins as a single component control in the near physiological 10 mM HEPES buffer to follow network assembly and evolution in real time and bridge between our previous detailed imaging of purified mucins and the ex vivo preocular fluid. To emphasise the differences between these two systems and to assay the contribution of companion molecules to the structure of tears, we imaged the integration of mucins into both an impression and a pure

Abbreviations: AFM, atomic force microscopy; DDT, dithiothreitol; DSU, dithiobis(succinimidylundecanoate).

mucin network. Finally, we disrupted intramolecular architecture to determine whether either system maintains its structure in the absence of disulphide intra- and intermolecular linked mucin polymers.

METHODS

Atomic force microscopy has been successfully used to refine the understanding of mucin architecture, conformation, and interactions.[14 15 20–22] To further exploit the advantages of this methodology we have developed a system for in situ real time imaging of mucins in an aqueous environment with no washing or drying steps in the protocol (Brayshaw *et al*, unpublished data). This technique enables visualisation and quantification of early stages of molecular adsorption and of molecular enzymic manipulation in situ.

The AFM (MultiMode, Veeco, Santa Barbara, CA, USA), fitted with a fluid cell, was operated in an intermittent contact ''tapping'' mode in liquid, allowing the preocular fluid and mucins to be imaged in their native hydrated state. Typically the triangular cantilever (a microfabricated silicon nitride construction of length 100 μm and thickness 0.7 μm with an integrated imaging tip) will resonate at about 8 kHz with an amplitude around 10 nm. As it taps the surface at the bottom of each oscillation cycle, the change in amplitude caused by the mechanical interaction with the sample is monitored, and used to build a three dimensional map of the surface.[13]

Imaging the preocular fluid and pure mucin assembly

To obtain a sample of the preocular fluid we used impression cytology[23 24] with freshly cleaved mica as a support. The impression was collected by pressing very lightly on the lower tarsal conjunctiva of a normal volunteer. The sample was immediately flooded with imaging buffer, 10 mM HEPES pH 7.4, 630 Ω, and mounted in the liquid cell of the AFM.

For the controlled assembly of single component networks, the positively charged binding surface was prepared by depositing a self assembled monolayer of 11, 11′-dithiobis(succinimidylundecanoate) (DSU)[25] on template-stripped gold prepared following the method of Hegner *et al*.[26] Immediately before use, the mica template was mechanically stripped using a scalpel to expose the atomically flat gold layer.

For dynamic AFM imaging 5 μl aliquots of purified mucin, approximately 10% of liquid surrounding the sample, were injected into the liquid cell while scanning, using a gel loading tip. If needed, imaging buffer was added in the same way. All imaging and interactions were followed therefore at the same ionic strength (that of the surrounding buffer) and a pH of 7.4, similar to that of tears.

The cantilevers were oscillated at a resonance frequency of 8 kHz. Using the resonance control technology of the ActivResonance Controller (Infinitesima, Bristol, UK), we increased the Q-factor of the cantilever, or ''sharpened'' the resonance, thus improving lateral resolution. All preocular fluid images reported in this paper were obtained using this Q-control.

Mechanical degradation

Switching from an oscillatory intermittent contact mode at the smallest force compatible with imaging to a mode of permanent contact between tip and sample, introduces tangential shear forces in addition to the ever present normal forces. These shear forces during sample scanning lead to frictional interactions and sample disruption. We used these destructive forces in a controlled fashion to excavate a hole in the gel in order to measure its thickness: the force was increased to 10 nN, while the scan rate was increased by an order of magnitude to 20 lines per second.

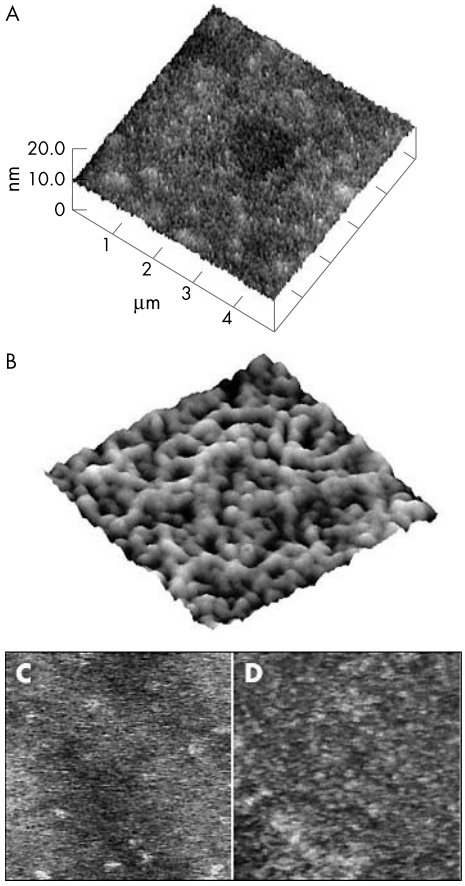

Figure 1 (A) A 5×5 μm scan of the preocular gel surface. Height is coded in grayscale; lighter shades indicate higher features. The lower area in the centre bears the imprint of a previous scan. (B) A 250×250 nm image of the macromolecular assembly of purified mucins. The molecules appear entangled, densely but irregularly spaced, yielding an image qualitatively similar to that of an agarose gel. (C and D) To show the effect of resonance feedback on image quality, the same 2.25 μm^2 area of preocular fluid was scanned by tapping under liquid, without (C) and with (D) the use of Q-control. The vertical Z range in both images is 0–5 nm (black to white).

Chemical degradation

Control of the imaging environment extends to the ability to introduce reagents that will interact with the sample. One such reagent is dithiothreitol (DTT) (Sigma, Poole, UK), which is used to cleave disulphide bonds. A 2 mM solution of DTT was added to the liquid surrounding the sample during AFM imaging and the resulting surface rearrangements were imaged in tapping mode with resonance control. Imaging was continued for some time thereafter to determine the state of the mucin molecules and of the preocular fluid.

Analysis

The three dimensional data set of an AFM image may be analysed in a number of ways. One approach is to look at the variation in image height along a line drawn across the image, the so-called line profile. The variation in height can be analysed statistically by using the root mean square roughness, which takes the data, pixel by pixel, and calculates the variation of each point from the mean datum level. This calculation may also be carried out on an area. The most complex method considered here is that of bearing analysis, which yields information on the variation in spatial distribution of height across a whole image. Starting from the highest pixel in the digital image, it is possible to plot a distribution curve, showing the proportion of the surface at a

certain height below the global maximum height. Height of imaged features is the most accurate parameter that can be quantified from a topographic image, as long as the size and shape of the tip are not so great as to prevent proper sampling of the surface, and that the tip is not contaminated with surface material. The ability to image single molecules on a macromolecular substrate (and not a flat mica substrate), as described below, would indicate that the tip is suitably sharp. The use of Q-control to reduce greatly the tapping force, and hence the deformation, means that we have greatly improved resolution and can measure dimensions with more confidence than would otherwise be the case.

Mucins extracted from human cadaveric conjunctival tissue were purified by sequential Caesium chloride gradient centrifugations with 4 M and 0.5 M guanidine hydrochloride. The largest molecules, excluded on Sepharose CL2B, within the classical isopycnicity of mucins, were used in this study. The mucins were exhaustively dialysed against imaging buffer.

RESULTS

Native preocular fluid and pure mucin network

Atomic force microscopy produces a three dimensional image of a surface. The impressions obtained from lower tarsal conjunctiva did not contain any cells or cell fragments, as expected from impressing with minimal pressure. A typical 2.25 μm^2 area is shown in fig 1A. The surface is flat; the rugosities are less than one nanometre. Q-control results in a lateral resolution better than 5 nm. A higher resolution three dimensional image of a 625 nm^2 area of the purified mucin network (fig 1B), reveals entangled molecules with irregular pores between them as expected from a fluid with a low solid component—for example, a gel. Note the beaded appearance of the individual mucin molecules, similar to their topography when imaged attached to a surface and at the highest resolution.

The outcome of Q-control on imaging the tear film is a striking increase in resolution in the AFM image as seen in the two scans of the same portion of impression surface shown without (fig 1C) and with resonance control (fig 1D).

Time series of images

To obtain the pure mucin assembly shown in figure 1B, we first ensured that the DSU gold substrate and imaging buffer were free from organic contaminants (fig 2A). Changes in surface features are observed within two minutes of injection of the pure mucins (fig 2B). The ringed areas of figure 2 A–D represent the same feature, as the scan area shifted slightly during imaging. The individual polymers adhering could be visualised for the entire duration of the experiment, as they attached either to the substrate or to already adherent molecules, forming a mat like network after repeated injection of mucins (fig 2D–N). Two further aliquots of mucin were injected at 40.4 minutes (fig 2F) and 82.3 minutes (fig 2K).

The volume of material deposited during the last 80 minutes of the experiment increased by more than 30% (fig 3A) whereas the average roughness decreased by one third (fig 3B), suggesting rearrangement of the molecules on the surface during the process of adsorption of new molecules from the surrounding buffer. Figure 3B indicates that the injection of mucins caused an initial increase in surface roughness, as expected when molecules adhere randomly to empty spaces on the substrate. That mucin molecules were able to explore the network is shown in figure 4, where a single molecule was followed in consecutive high magnification images. Changes in its profile and arrangement on the surface are clearly seen. Molecular rearrangement leading to a decrease in surface roughness suggests infill of surface features.

While imaging the preocular impression at high resolution with the Q-control operating, 5 µl amounts of dilute mucin solution were injected into the imaging environment. Over the course of 60 minutes, the same area was imaged while two injections of mucin were carried out. The sequence of images is shown in figure 5. The images were all recorded under identical conditions and all share the same 0–5 nm height scale. The images, although clearly of the same area of the impression, show qualitative and quantitative changes in structure. The most obvious initial observation would be an increase with time in the localised high features that decorate

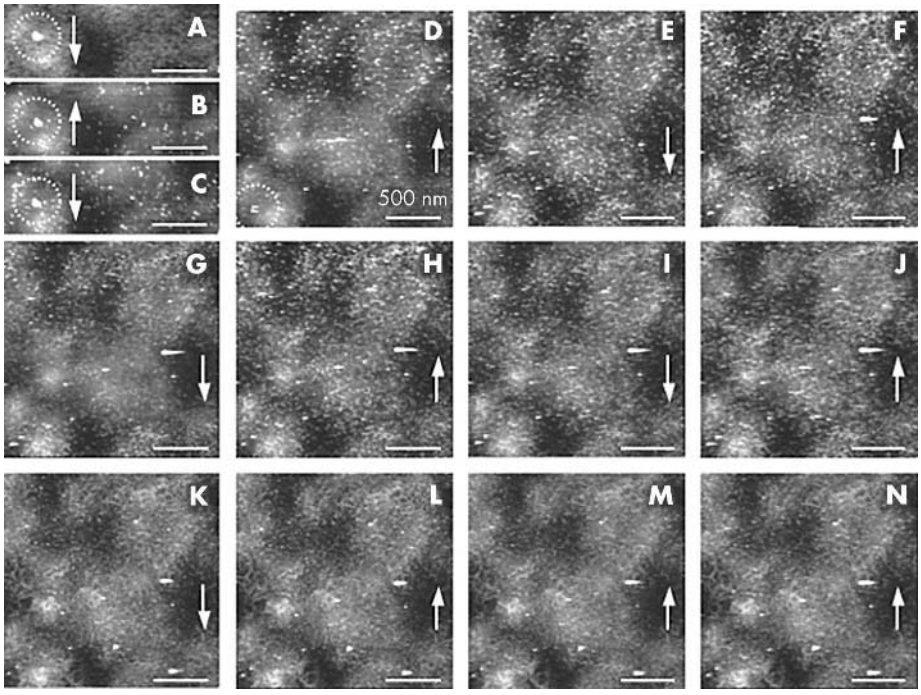

Figure 2 Repeated addition of pure mucins into the imaging buffer resulted in the formation of a mucin network on the DSU. Arrows indicate the slow scan direction. (A) Initial scan in 10 mM HEPES buffer. An aliquot of 5 µl mucin was injected at the end of this scan; time, t = 0; (B) t = 2.1 min; (C) t = 4.6 min; (D) t = 19.5 min; (E) t = 23.7 min; (F) t = 40.4 min, second addition of mucin at end of this scan; (G) t = 44.6 min; (H) t = 48.8 min; (I) t = 53.0 min; (J) t = 57.2 min; (K) t = 82.3 min, third mucin addition at end of this scan; (L) t = 86.5 min; (M) t = 94.9 min; (N) t = 103.3 min. In all images the Z range is 0–6 nm, and the scale bar represents 250 nm and the arrow denotes the slow scan axis.

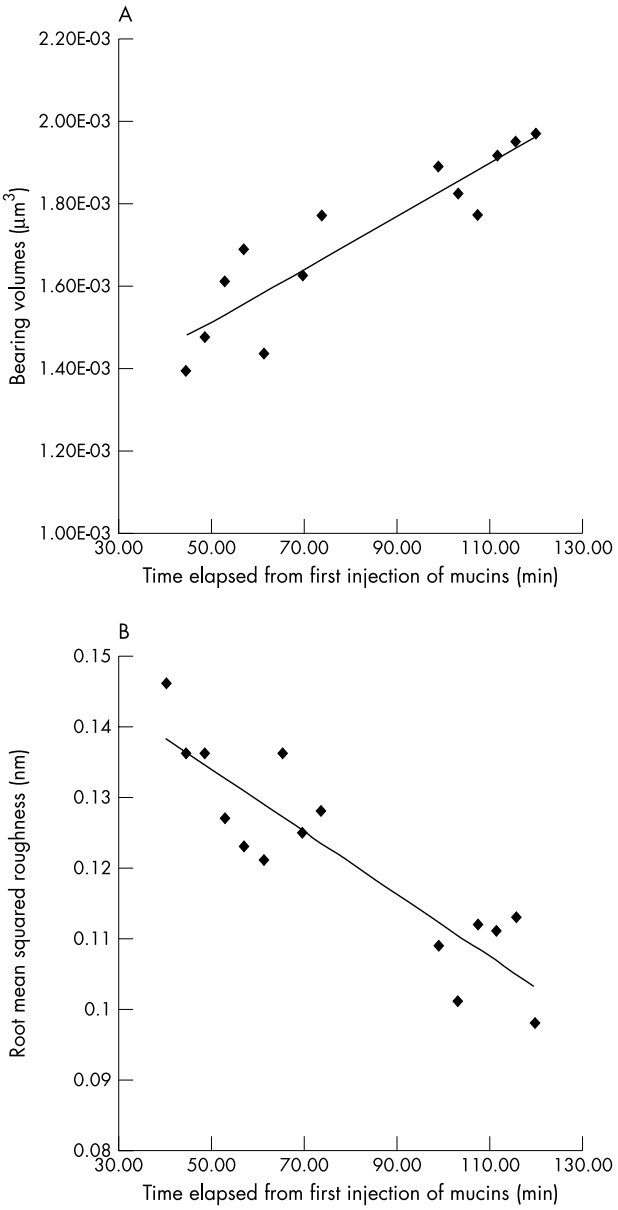

Figure 3 Analysis of image data in figure 2. (A) The increase in bearing volume or ''material volume'' of the same 1×1 µm area as the surface evolved during the mucin adsorption. (B) The corresponding evolution of surface roughness, evaluated as root mean square roughness, from the same area of the sample.

the surface, apparent as white dots in the images. These increase in size and number with time.

In these images scanned at high resolution, differences between the highest peaks and lowest valleys were of the order of 0.2–0.4 nm, much smaller than the wavelength of visible light. The roughness of the impression surface responded to mucin injection with an upward trend in root mean square, from 0.075 nm to 0.1 nm (fig 6A). Unlike the global estimates, the roughness calculated for the line linking the two prominent features highlighted in figure 5, decreased with time, suggesting a local filling in of low height features as shown in figure 6A. Figure 6B shows clearly that the surface is undergoing dynamic changes in the distribution of material, changes that are also reflected in the respective bearing volumes at each scan.

The fact that the image was not lost during more than one hour of continuous scanning indicates that none or very little impression material dissolved into the buffer or adsorbed to the tip.

Mechanical manipulation of impression

We purposefully excavated the gel by increasing the force above 10 nN for 1 minute and scanning a small area at 20 lines per second, rather than the normal 1–2 lines per second. Restoring the AFM to its normal operating conditions—slow scanning speed and with resonance control—we visualised the results of this mechanical manipulation, as shown in figure 7A. An accumulation of material can be observed around a low height area. Line profiles of this area revealed a cavity, indicating that material had been removed leaving the original mica surface exposed. The height difference between the impression surface at some distance from the mechanically altered site and the bottom of the cavity, defined by the two arrows in figure 7B, was 10.8 nm, consistent with a small number of molecules.

Chemical manipulation of the imaged structures

Addition of DTT to the imaging buffer had an almost immediate effect (fig 8) which shows a 1.5 µm AFM scan of the impression surface. The image on the right (fig 8B) was recorded immediately following figure 8A. The bobbly appearance of the pre-DTT image is still present in the first few (bottom) lines of the right image, until the DTT injection. The injection is evident from the streaky lines of the image (arrowed). Comparing the full images, where circled features define equivalent points, it can be seen that the action of the DTT has resulted in the loss of surface material, and a clearer exposure of previously barely protruding features, starting between 30 and 201 seconds after injection. In this image (fig 8B) scanning was collected from the bottom to top. Further chemically controlled depolymerisation of mucins can be seen at the top of figure 8B, caused by the second injection of DTT. Subsequent imaging was impossible because of loss of surface material. The tip may also have become ''contaminated'' by detached material—that is, gel fragments might have bound or come to rest on it—resulting in artefactual doubling of imaged features. Similar results were obtained with control purified mucin gels (fig 8C).

DISCUSSION

Although large secreted mucins have been shown to create gels, and furthermore gels with structure that varies according to location,[27] the concentration of pure mucins required to create a gel has been estimated as much larger than physiological.[18] The existence of very hydrated gels on eyes or in saliva is therefore likely to be the result of the interaction between different chemical entities.[18] Here we have applied atomic force microscopy to compare the behaviour of mucins contained in a multimolecular, multicomponent assembly, as found on the ocular surface, to that of a one component macromolecular assembly built up from purified ocular mucins.

Impression cytology is well established as a technique of sampling preocular fluid and superficial cells, the efficiency of collecting the latter depending on the pressure applied to the ocular surface. We have used this technique to collect a very thin film of preocular fluid, free of cells. Given a sufficiently thin layer, features on the surface of the sample can be gleaned by imaging its underside, which is important in this experiment, as the superficial aspect of the preocular film is apposed to the carrying support. The thickness measurement following mechanical manipulation of the ocular fluid impression, which corresponds to a maximum of 10 molecular diameters,[14] supports the claim that the AFM had access to surface features of the preocular material collected by impression cytology. Images of this fluid are

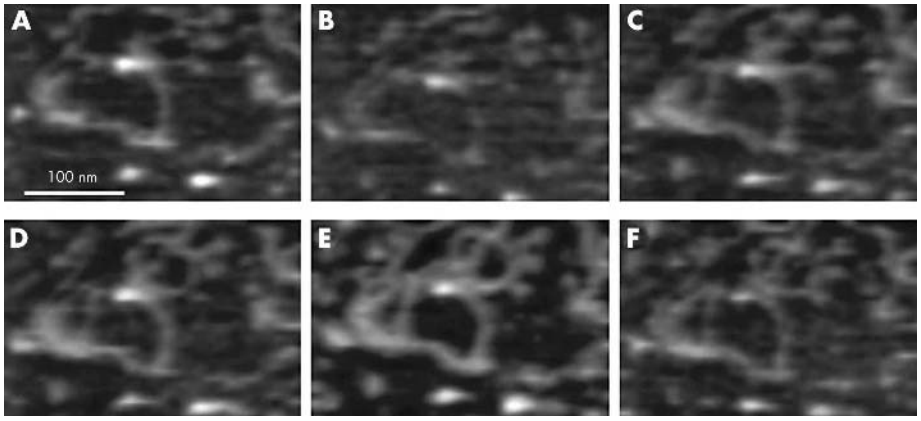

Figure 4 Diffusional movement of a single mucin molecule on macromolecular mucin assembly is highlighted in consecutive images (A–F), and indicates that mucins are able to explore the surface while remaining in part attached.

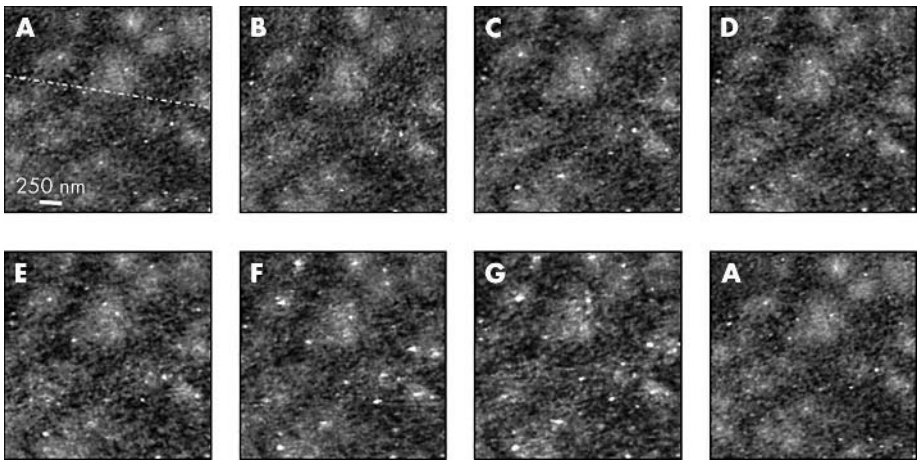

Figure 5 A panel showing the same 2.34×2.34 μm area of the preocular impression imaged over the course of 50 minutes. All images have a Z range of 0–5 nm. The dotted line in image (A) represents the line profile used for roughness measurement. Image (A) is repeated in the panel to aid comparison of surfaces ''before'' and ''after'' mucin addition. (A) Initial scan, time, t=0 at the end of this scan; (B) t=8.5 min, an aliquot of mucin solution was added during this scan; (C) t=17.1 min; (D) t=25.6 min; (E) t=34.1 min; (F) t=42.6 min, a second aliquot of mucin was added during this scan; (G) t=51.1 min.

consistent with a gel whose surface features are of sizes ignored by visible light, for being much smaller than the wavelengths in the visible spectrum, thus providing an optical surface free of refraction artefacts. It is interesting to note that the preocular fluid in vitro is much rougher than a pure mucin network assembled in vitro.

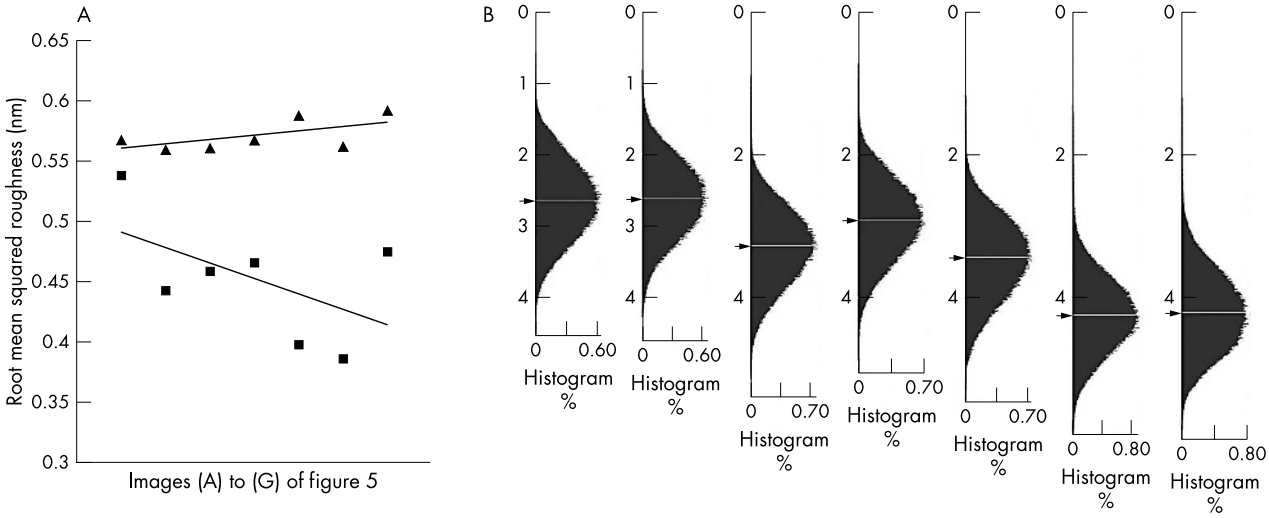

Figure 6 (A) Roughness data for the images A–G of figure 5. The top set of points (black triangles) are the data for the global image in each case, and show overall roughness remaining fairly constant; the lower set (grey squares) are the roughness values obtained along the same spatial line in each successive image, showing a decrease with time (and the addition of mucins to the impression surface), and suggesting infill of some areas. (B) Bearing volume curves for each of the images A–G in figure 5. Each curve shows the distribution of surface area covered as a function of height below the tallest point in the specific image. From the bearing analysis of the same 5.5 μm^2 area in consecutive images, it becomes apparent that the volume of material increases as the centre of the distribution shifts to higher values.

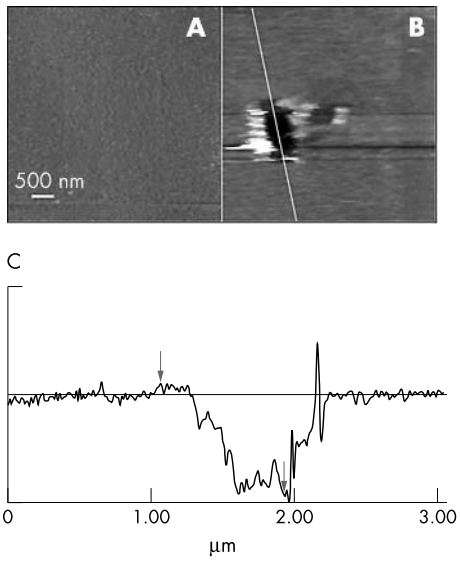

Figure 7 (A and B) ''Before'' and ''after'' images of a 5×5 µm area of the impression surface. The scan size is 5×5 µm and the vertical Z range is 0–20 nm. (B) The force between tip and sample, kept below the threshold for disrupting the sample when imaging, was deliberately increased to remove the impression material from a small area and expose the underlying mica. (C) From the line profile taken along the diagonal line in (B), the thickness was measured as 10.8 nm. Note that the material removed from the cavity was deposited at its edges.

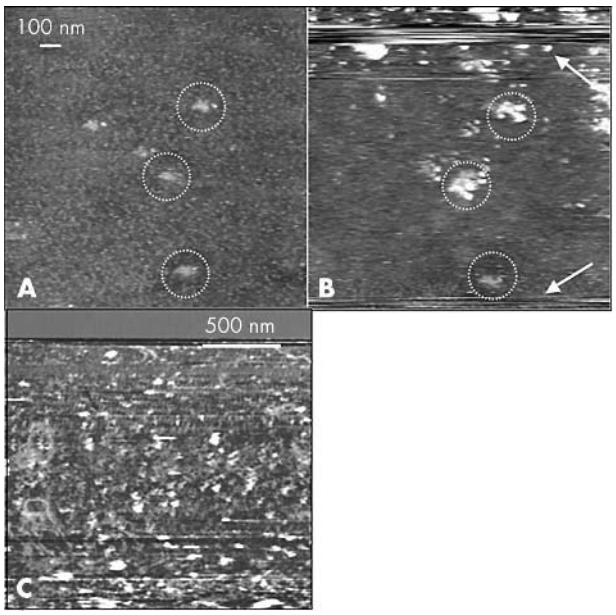

Figure 8 ''Before'' and ''after'' images showing the effect of addition of a 10 mM DTT solution to the imaging buffer. (A) This image of the preocular impression was collected before the injection, scan direction is from top to bottom. (B) The injections of DTT are reflected in the streaked lines at the bottom, and at the top of the impression (see arrows). Scan direction is bottom to top. The DTT resulted in an alteration of surface features. The circled areas in both images are the same prominent features imaged before and after the injection of DTT. They are higher after the introduction of the reducing agent. The scan size is 1.5×1.5 µm and the vertical Z range is 0–15 nm. (C) Image of the pure mucin network (as in fig 2N) immediately after the injection of DTT. Note the large increase in surface irregularity.

The evolution of the pure mucin macromolecular assembly, where a decrease in height differences over the surface was observed as the volume of material deposited increased, can be explained by mucins adhering to the unoccupied tethering surface. This random sequential adsorption leads to an initial increase in surface roughness. The further substantial decrease in surface roughness suggests molecular rearrangements of subsequently deposited entities. Conformation alterations of an individual molecule indicate that such rearrangements are possible. Furthermore, the image of the mature network shows that molecules are not confined to the first surface they encounter but will penetrate into the bulk of the adsorbed structure, suggesting entanglements, and therefore movement, within the volume of the mucin gel like network.

Roughness fluctuations in response to injection of pure mucins onto the preocular gel are also consistent with molecular rearrangements. This is further supported by infill of low height features between persistent local maxima, as shown in the line profile analysed here. It is noteworthy that fluctuations in the multicomponent gel are smaller than in the single component macromolecular structure, although the mechanisms leading to this are still obscured by the complexity of intermolecular interactions. Another feature that unifies the two systems studied here is the devastating effect of disulphide bond breaking on the architecture of the imaged structures. When individual mucins are reduced to smaller polymers, or when disulphide bond cleavage reduces the cross linking of the network, molecules leave the assembly and become dissolved in the imaging buffer where they attach to the cantilever causing the image to be lost. This rate of dissolution is significantly greater than the rate of introduction of mucins to the surfaces. Similarly, substantial amounts of impression material were lost after the introduction of the reducing agent, where none or very little had been lost during the hour long scanning that preceded it. Polymeric mucin, therefore, gelling through disulphide bond cross linking, prevents or retards loss of material from the preocular gel into the surrounding solution. Mucin interactions are thus required for the stability of the fluid coating the ocular surface.

Authors' affiliations

M Berry, Ophthalmology, University of Bristol, Bristol Eye Hospital, Bristol, UK
D Brayshaw, T J McMaster, Nanostructures and Microstructures Group, University of Bristol, H H Wills Physics Laboratory, Bristol, UK

Correspondence to: Dr M Berry, University of Bristol, Bristol Eye Hospital, Lower Maudlin Street, Bristol BS1 2LX, UK; mon.berry@bristol.ac.uk

Accepted 7 March 2004

REFERENCES

1 **Dilly PN**. Structure and function of the tear film. *Adv Exp Med Biol* 1994;**350**:239–47.
2 **Prydal JI**, Campbell FW. Study of precorneal tear film thickness and structure by interferometry and confocal microscopy. *Invest Ophthalmol Vis Sci* 1992;**33**:1995–2005.
3 **King-Smith PE**, Fink BA, Fogt N, *et al*. The thickness of the human precorneal tear film: evidence from reflection spectra. *Invest Ophthalmol Vis Sci* 2000;**41**:3348–59.
4 **Creech JL**, Do LT, Fatt I, *et al*. In vivo tear-film thickness determination and implications for tear-film stability. *Cur Eye Res* 1998;**17**:1058–66.
5 **Goto E**, Tseng SCG. Differentiation of lipid tear deficiency dry eye by kinetic analysis of tear interference images. *Arch Ophthalmol* 2003;**121**:173–80.
6 **Rieger G**. The importance of the precorneal tear film for the quality of optical imaging. *Br J Ophthalmol* 1992;**76**:157–8.
7 **Hansma HG**, Pietrasanta LI, Auerbach ID, *et al*. Probing biopolymers with the Atomic Force Microscope: a review. *J Biomater Sci Polym Ed* 2000;**11**:675–83.
8 **Corfield AP**, Carrington SD, Hicks SJ, *et al*. Ocular mucins: purification, metabolism and function. *Prog Ret Eye Res* 1997;**16**:627–56.

9 **Gipson IK**, Inatomi T. Mucin genes expressed by the ocular surface epithelium. *Prog Ret Eye Res* 1997;**16**:81–98.
10 **Jumblatt JE**, Cunningham LT, Li Y, *et al*. Characterization of human ocular mucin secretion mediated by 15(S)-HETE. *Cornea* 2002;**21**:818–24.
11 **Manabe T**. Combination of electrophoretic techniques for comprehensive analysis of complex protein systems. *Electrophoresis* 2000;**21**:1116–22.
12 **Viovy J-L**. Electrophoresis of DNA and other polyelectrolytes: Physical mechanisms. *Rev Mod Phys* 2000;**72**:813–72.
13 **Moller C**, Allen M, Elings V, *et al*. Tapping-mode atomic force microscopy produces faithful high-resolution images of protein surfaces. *Biophys J* 1999;**77**:1150–8.
14 **McMaster TJ**, Berry M, Corfield AP, *et al*. Atomic force microscopy of the submolecular architecture of hydrated ocular mucins. *Biophys J* 1999;**77**:533–41.
15 **Round AN**, Berry M, McMaster TJ, *et al*. Heterogeneity and persistence length in human ocular mucins. *Biophys J* 2002;**83**:1661–70.
16 **Tamayo J**, Humphris ADL, Miles MJ. Piconewton regime dynamic force microscopy in liquid. *App Phys Lett* 2000;**77**:582–4.
17 **Tamayo J**, Humphris AD, Malloy AM, *et al*. Chemical sensors and biosensors in liquid environment based on microcantilevers with amplified quality factor. *Ultramicroscopy* 2001;**86**:167–73.
18 **Bromberg LE**, Barr DP. Self-association of mucin. *Biomacromolecules* 2000;**1**:325–34.
19 **Raynal BD**, Hardingham TE, Thornton DJ, *et al*. Concentrated solutions of salivary MUC5B mucin do not replicate the gel-forming properties of saliva. *Biochem J* 2002;**362**:289–96.
20 **Berry M**, McMaster TJ, Corfield AP, *et al*. Exploring the molecular adhesion of ocular mucins. *Biomacromolecules* 2001;**2**:498–503.
21 **Brayshaw DJ**, Berry M, McMaster TJ. Optimisation of sample preparation methods for air imaging of ocular mucins by AFM. *Ultramicroscopy* 2003;**97**:289–96.
22 **Shi L**, Caldwell KD. Mucin adsorption to hydrophobic surfaces. *J Colloid Interface Sci* 2002;**224**:372–81.
23 **Egbert PR**, Lauber S, Maurice DM. A simple conjunctival biopsy. *Am J Ophthalmol* 1977;**84**:798–801.
24 **Hareuveni T**, Maurice DM. Short-term reproducibility of impression cytology. *Cornea* 1994;**13**:250–2.
25 **Wagner P**, Hegner M, Kernen P, *et al*. Covalent immobilization of native biomolecules onto Au(111) via N-hydroxysuccinimide ester functionalized self-assembled monolayers for scanning probe microscopy. *Biophys J* 1996;**70**:2052–66.
26 **Hegner M**, Wagner P, Semenza G. Ultralarge atomically flat template-stripped Au surfaces for scanning probe microscopy. *Surf Sci* 1993;**291**:39.
27 **Atuma C**, Strugala V, Allen A, *et al*. The adherent gastrointestinal mucus gel layer: thickness and physical state in vivo. *Am J Physiol Gastrointest Liver Physiol* 2001;**280**:G922–29.